Citation: CPT Pharmacometrics Syst. Pharmacol. (2014) 3, e141; doi:10.1038/psp.2014.39

www.nature.com/psp

ORIGINAL ARTICLE

Identifying Determinants of EGFR-Targeted Therapeutic Biochemical Efficacy Using Computational Modeling

CS Monast[1] and MJ Lazzara[1,2]

We modeled cellular epidermal growth factor receptor (EGFR) tyrosine phosphorylation dynamics in the presence of receptor-targeting kinase inhibitors (e.g., gefitinib) or antibodies (e.g., cetuximab) to identify systematically the factors that contribute most to the ability of the therapeutics to antagonize EGFR phosphorylation, an effect we define here as biochemical efficacy. Our model identifies distinct processes as controlling gefitinib or cetuximab biochemical efficacy, suggests biochemical efficacy is favored in the presence of certain EGFR ligands, and suggests new drug design principles. For example, the model predicts that gefitinib biochemical efficacy is preferentially sensitive to perturbations in the activity of tyrosine phosphatases regulating EGFR, but that cetuximab biochemical efficacy is preferentially sensitive to perturbations in ligand binding. Our results highlight numerous other considerations that determine biochemical efficacy beyond those reflected by equilibrium affinities. By integrating these considerations, our model also predicts minimum therapeutic combination concentrations to maximally reduce receptor phosphorylation.
CPT Pharmacometrics Syst. Pharmacol. (2014) **3**, e141; doi:10.1038/psp.2014.39; published online 15 October 2014

For various malignancies, small-molecule inhibitors and antibodies that antagonize the function of oncogenic receptor tyrosine kinases are in use or in clinical trials. For the epidermal growth factor receptor (EGFR), ATP analog kinase inhibitors including gefitinib and erlotinib are approved for non–small cell lung carcinoma and pancreatic cancer,[1,2] and the ligand-competitive monoclonal antibody cetuximab is approved for head and neck and colorectal cancers.[3] While these therapeutics target the same receptor, there may be important determinants of their abilities to antagonize EGFR-initiated signaling beyond the competitive binding processes in which they participate, and those determinants may be unique for different therapeutic classes owing to the different steps of the receptor phosphorylation process at which the therapeutics act. Identifying such determinants may aid in the rational design of next-generation therapeutics targeting EGFR and could provide insight into the differential effectiveness of these therapeutics *in vitro* and *in vivo* (e.g., refs. 4–6).

Computational modeling represents a useful approach for systematically identifying processes that determine the abilities of therapeutics to antagonize EGFR signal-initiating capacity. Of course, a number of detailed kinetic models of EGFR signaling have been developed with varying levels of complexity (e.g., refs. 7–11). Surprisingly, none of these has been utilized to explore directly the determinants of the ability of different classes of EGFR-targeted therapeutics to interrupt EGFR-initiated signaling. For EGFR and other receptor tyrosine kinases, the well-known model of Cheng and Prusoff[12] has also been invoked to make inferences about therapeutic efficacy (e.g., ref. 13), but the simplicity of this model prevents a full analysis of all receptor-level processes that may influence therapeutic effects (e.g., receptor trafficking).

Here, we build upon a previous model of EGFR phosphorylation dynamics to identify systematically the key receptor-level processes that enable gefitinib and cetuximab to antagonize EGFR phosphorylation in the cellular context. We focus on determinants of EGFR phosphorylation since that is the initial step enabling EGFR to generate downstream signaling. We find that the processes that determine biochemical efficacy (defined here as ability to reduce EGFR tyrosine phosphorylation) extend beyond those involved in equilibrium EGFR-therapeutic binding and differ by therapeutic and ligand. For example, gefitinib and cetuximab are predicted to be more effective when EGFR activation is driven by amphiregulin (AR) than by epidermal growth factor (EGF) due to differences in affinity and time scales for receptor occupancy. EGFR tyrosine dephosphorylation rate is predicted to be a preferentially important determinant of gefitinib biochemical efficacy, while ligand binding rate is a preferentially important determinant of cetuximab biochemical efficacy, again due to differences in relevant process time scales. Our model also predicts how gefitinib and cetuximab can be most efficiently combined to reduce receptor phosphorylation maximally but minimize drug concentrations and redundant effects.

RESULTS

Inhibition of receptor phosphorylation by gefitinib or cetuximab

The model considers the rate processes leading to EGFR phosphorylation in cell surface and interior compartments (**Figure 1a**). See **Table 1** for definitions and values of rate parameters. Reversibility of all processes is considered, allowing gefitinib and cetuximab to antagonize EGFR phosphorylation not only for already drug-bound receptors but through other rate processes, such as prolonging the

[1]Department of Chemical and Biomolecular Engineering, University of Pennsylvania, Philadelphia, Pennsylvania, USA; [2]Department of Bioengineering, University of Pennsylvania, Philadelphia, Pennsylvania, USA. Correspondence: MJ Lazzara (mlazzara@seas.upenn.edu)

Received 28 May 2013; accepted 29 July 2014; published online 15 October 2014. doi:10.1038/psp.2014.39

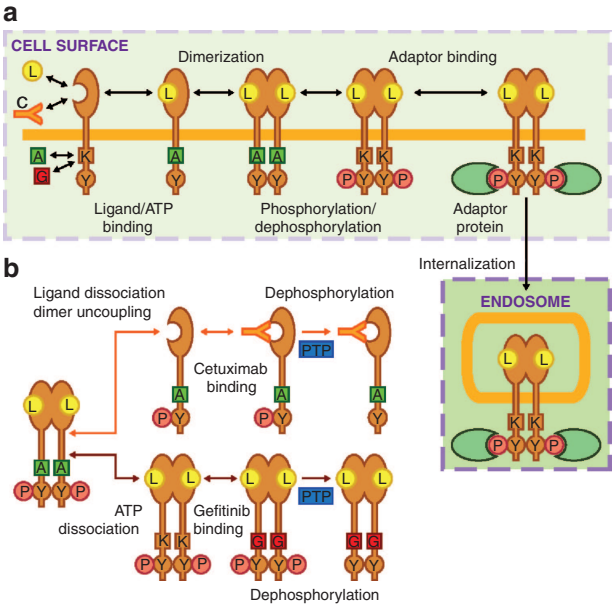

Figure 1 Model topology of processes leading to epidermal growth factor receptor (EGFR) phosphorylation and therapeutic inhibition of this process. (**a**) Ligand (*L*) and cetuximab (*C*) compete for binding to the EGFR extracellular domain while ATP (*A*) and gefitinib (*G*) compete for binding to the EGFR kinase domain (*K*). Ligand binding promotes EGFR dimerization and ATP-dependent phosphorylation (*P*) of cytoplasmic tyrosines (*Y*), enabling receptor binding to intracellular adaptor proteins (e.g., GRB2). EGFR-GRB2 binding permits EGFR internalization. (**b**) Gefitinib and cetuximab mediate reductions in the phosphorylation of dimerized and phosphorylated EGFR through different mechanisms. ATP dissociation from EGFR allows gefitinib to bind, prolonging the time the receptor remains dephosphorylated after being acted upon by protein tyrosine phosphatases (PTP). Cetuximab can bind phosphorylated receptors once they uncouple from dimers and ligands dissociate, which slows further rounds of ligand binding and dimerization and prolongs the time the receptor remains dephosphorylated after being acted upon by PTPs.

dephosphorylated receptor state after receptors are acted upon by protein tyrosine phosphatases (Figure 1b). Throughout these results, we report therapeutic biochemical efficacy in terms of an IC_{50}, defined as the therapeutic concentration required to reduce steady EGFR phosphorylation to half its value in the absence of therapeutic.

We begin by simulating inhibition curves for 10 ng/ml (1.6 nmol/l) EGF or equimolar AR for all ligand/therapeutic combinations (Figure 2a). For cetuximab and gefitinib, the predicted IC_{50} in the presence of EGF exceeds that for AR by roughly an order of magnitude (Figure 2b). This occurs, in part, because AR's lower affinity reduces receptor occupancy and the dimerization driving force. For either ligand, the predicted IC_{50} is larger for gefitinib than cetuximab. This occurs, in part, because the particular combinations of species concentrations and binding kinetics disfavor gefitinib's competition with ATP more than cetuximab's with ligand. Additional factors contribute to these differences, as will be discussed. To account for different ligand affinities, we repeated the analysis for a 100-fold increase in AR concentration (Figure 2c). This reduces, but does not eliminate, predicted IC_{50} differences (Figure 2d).

Table 1 Model parameters

Parameter	Description	Value	Source
$k_{L,fs}$ ((μmol/l)$^{-1}$ * min^{-1})	Ligand binding to EGFR, forward, surface	3.1×10^{2}	46
$k_{L,rs}$ (min^{-1})[a]	Ligand binding to EGFR, reverse, surface	8.0×10^{-1}	K_D[21]
$k_{L,fi}$ (endosome·min^{-1})	Ligand binding to EGFR, forward, endosome	3.1×10^{-4}	21
$k_{L,ri}$ (min^{-1})[a]	Ligand binding to EGF, reverse, endosome	6.6×10^{-1}	21
$k_{A,f}$ ((μmol/l)$^{-1}$ * min^{-1})	ATP binding to EGFR, forward	1.0×10^{5}	27
$k_{A,r}$ (min^{-1})	ATP binding to EGFR, reverse	1.1×10^{7}	27
$k_{g,f}$ ((μmol/l)$^{-1}$ * min^{-1})	Gefitinib binding to EGFR, forward	1.0×10^{5}	27
$k_{g,r}$ (min^{-1})	Gefitinib binding to EGFR, reverse	2.1×10^{2}	27
$k_{c,f}$ ((μmol/l)$^{-1}$ * min^{-1})	Cetuximab binding to EGFR, forward	1.3×10^{1}	38
$k_{c,r}$ (min^{-1})	Cetuximab binding to EGFR, reverse	6.6×10^{-2}	38
$k_{G2,f}$ (cell·min^{-1})	GRB2 binding to EGFR, forward	3.8×10^{-4}	17
$k_{G2,r}$ (min^{-1})	GRB2 binding to EGFR, reverse	4.6×10^{2}	17
$k_{d,fs}$ (cell·min^{-1})	EGFR dimerization, forward, surface	6.7×10^{-4}	Calculated[27]
$k_{d,fi}$ (endosome·min^{-1})	EGFR dimerization, forward, endosome	2.7×10^{-3}	Calculated[27]
$k_{d,r}$ (min^{-1})	EGFR dimerization, reverse, unoccupied	1.0×10^{4}	K_D[47]
$k_{d,rL}$ (min^{-1})	EGFR dimerization, reverse, ligand-occupied	1.0×10^{-1}	48
k_{p} (min^{-1})	Phosphorylation, unoccupied dimer	2.7×10^{0}	49
$k_{p,L}$ (min^{-1})	Phosphorylation, ligand-occupied dimer	1.3×10^{1}	49
$k_{dp,s}$ (min^{-1})	Dephosphorylation, surface	5.3×10^{0}	fit
$k_{dp,i}$ (min^{-1})	Dephosphorylation, endosome	2.2×10^{0}	fit
k_{i} (min^{-1})	EGFR internalization	Varies	Calculated[27]
k_{x} (min^{-1})	Endosomal exit	4.0×10^{-2}	50
f_{rE}	Recycle fraction, EGF-occupied	5.0×10^{-1}	50
f_{r}	Recycle fraction, unoccupied	8.0×10^{-1}	50
[EGFR] (cell^{-1})	EGFR expression per cell	5.0×10^{4}	42
[GRB2] (cell^{-1})	GRB2 expression per cell	2.1×10^{5}	43
[ATP] (mmol/l)	Intracellular ATP concentration	1 mmol/l	44

[a]Values for EGF are shown. Dissociation rate constants for amphiregulin were set equal to these values multiplied by 100.
EGFR, epidermal growth factor receptor.

Effect of ligand and therapeutic binding kinetics on predicted IC_{50} values for gefitinib and cetuximab

Given that differences in ligand affinity do not fully explain predicted IC_{50} differences, we performed an analysis assuming constant affinities of ligand (based on EGF) and drug (gefitinib or cetuximab) but varying rate constants for ligand and drug binding and unbinding by an equal "cycling factor"

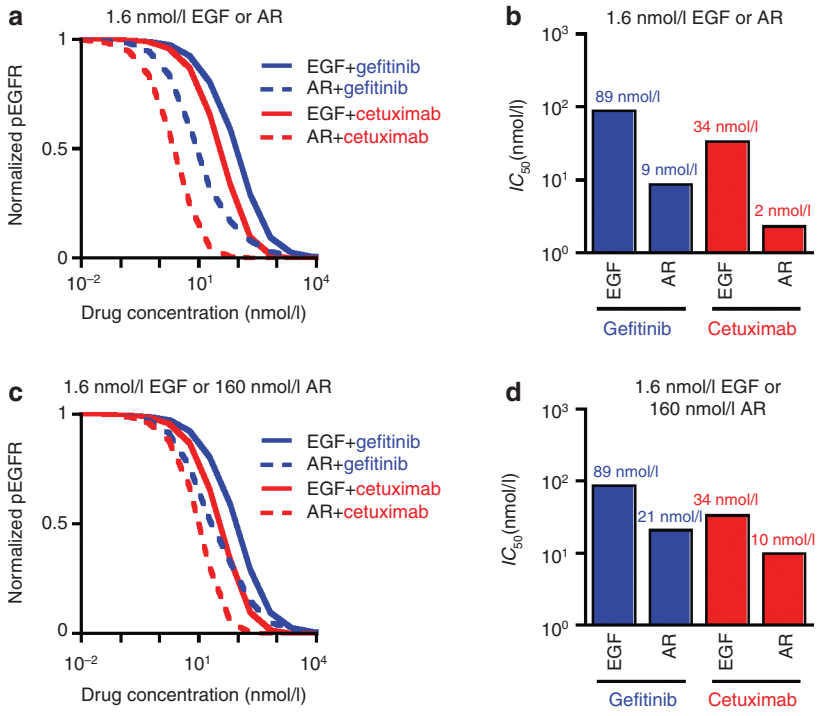

Figure 2 Predicted therapeutic IC_{50} values. (**a**) For a range of gefitinib or cetuximab concentrations and 1.6 nmol/l EGF or amphiregulin (AR), the amount of steady-state phosphorylated epidermal growth factor receptor (EGFR) (pEGFR) was computed and normalized to the amount of pEGFR in the absence of therapeutic. (**b**) From the data shown in panel (**a**), gefitinib and cetuximab IC_{50} values were calculated for each ligand/therapeutic pair. (**c** and **d**) Calculations in panels (**a**) and (**b**) were repeated for 160 nmol/l AR and compared to results for 1.6 nmol/l EGF.

(**Figure 3a**,**b**). Faster ligand cycling on and off the receptor generally reduces predicted gefitinib and cetuximab IC_{50}. For example, a 10-fold increase in EGF cycling from base values reduces gefitinib or cetuximab IC_{50} by ~25 or 40%, respectively. This occurs because of a reduced phosphorylation driving force as the time scale for ligand occupancy becomes similar or small compared to the time scale for ligand-bound receptors to become phosphorylated, as reflected by decreased EGFR phosphorylation in the absence of drugs with increasing ligand cycling (vertical grey scale bars in **Figure 3**).

Figure 3a,**b** also show predicted effects of changing gefitinib or cetuximab cycling. Sufficient decreases in gefitinib cycling reduce gefitinib IC_{50} (**Figure 3a**), consistent with the notion that irreversible EGFR kinase inhibitors are more effective than reversible inhibitors.[14] This occurs because the receptor is increasingly less likely to rephosphorylate as the time scale with which it remains inhibitor-bound increases. Consistent with this, sensitivity to gefitinib cycling decreases as EGFR cycling through phosphorylated and unphosphorylated states slows (**Figure 3c**). In contrast, cetuximab's biochemical efficacy is relatively insensitive to changes in cetuximab cycling (**Figure 3b**) because of competing effects. As cetuximab cycling increases, IC_{50} tends to decrease because cetuximab binds the receptor more slowly than ligand for the base parameters. That effect is offset, however, because the time scale for cetuximab dissociation from EGFR decreases and approaches that for receptor dephosphorylation as cetuximab cycling increases, which increases IC_{50}. The modest net effect of cetuximab cycling on IC_{50} can be eliminated by reducing receptor dimerization and uncoupling rates (**Figure 3d**) because cetuximab binding and dissociation steps are no longer rate limiting in the competitive processes described above that allow cetuximab cycling to influence IC_{50}. Not surprisingly, IC_{50} values are also reduced by this parameter alteration.

IC_{50} sensitivity analysis

To identify other processes that determine IC_{50}, we performed parameter sensitivity analyses. The predicted gefitinib IC_{50} in the presence of 1.6 nmol/l EGF is most sensitive to perturbations in parameters for ATP binding ($k_{A,f}$ and $k_{A,r}$), gefitinib binding ($k_{g,f}$ and $k_{g,r}$), EGFR phosphorylation ($k_{p,L}$), and EGFR dephosphorylation ($k_{dp,s}$ and $k_{dp,i}$) (**Figure 4a**). Sensitivity to perturbations in ATP and gefitinib binding is anticipated because these parameters control gefitinib/ATP competition. Sensitivity to changes in $k_{dp,s}$, $k_{dp,i}$, and $k_{p,L}$ arises because of the importance of receptor dephosphorylation and phosphorylation cycles in setting steady phosphorylation. The gefitinib IC_{50} in the presence of 1.6 nmol/l AR is sensitive to perturbations in ATP and gefitinib binding but relatively insensitive to perturbations in $k_{p,L}$, $k_{dp,s}$, and $k_{dp,i}$ because 1.6 nmol/l AR does not promote substantial dimerization or phosphorylation. For 160 nmol/l AR, the number of dimers present at steady-state increases >20-fold, and the model predicts increased sensitivity to perturbations in parameters for ligand-receptor association and dissociation ($k_{L,fs}$ and $k_{L,rs}$, respectively), $k_{p,L}$, $k_{dp,s}$, and $k_{dp,i}$.

For cetuximab, the IC_{50} in the presence of 1.6 nmol/l EGF ($IC_{50}^{E,c}$) is most sensitive to perturbations in $k_{L,fs}$ and $k_{L,rs}$, rate

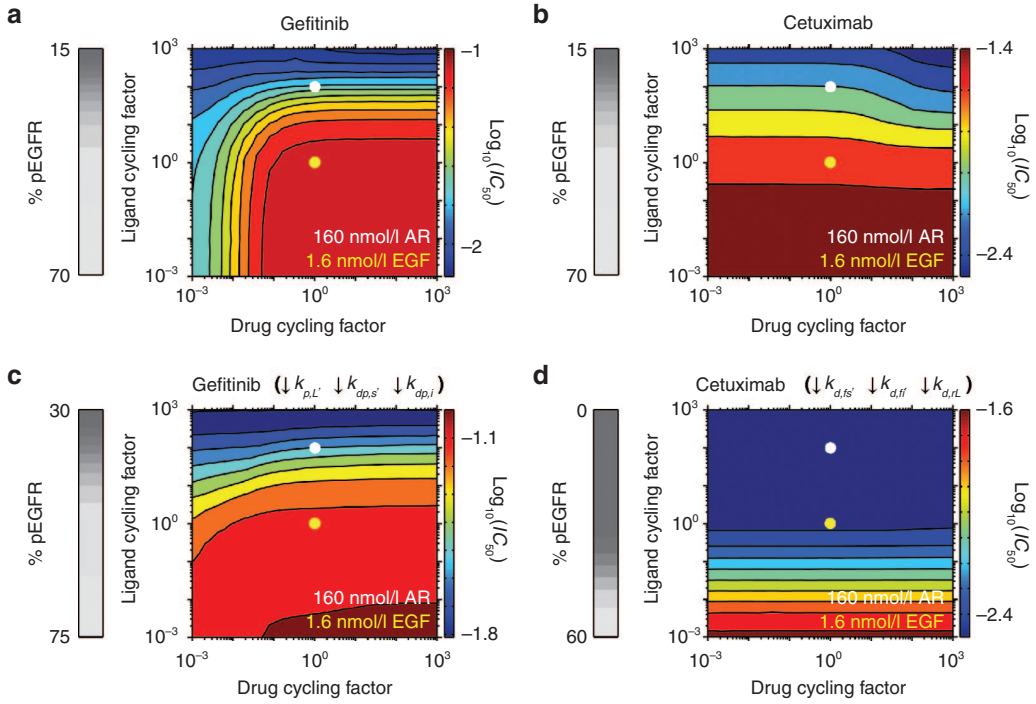

Figure 3 Effects of the rates of cycling of ligand or therapeutic binding and unbinding. Gefitinib and cetuximab IC_{50} values were calculated for the indicated fold-changes in ligand or drug cycling factor, a constant by which the ligand or drug association and dissociation rate constants are multiplied such that binding/unbinding rates change without altering affinities. Ligand cycling rates corresponding to 1.6 nmol/l epidermal growth factor (EGF) and 160 nmol/l amphiregulin (AR) are indicated by the yellow and white dots, respectively. 160 nmol/l AR is equivalent to 1.6 nmol/l EGF with a ligand cycling factor of 100 because AR is treated as dissociating from EGFR 100 times faster than EGF and the 100-fold greater AR concentration leads to a 100-fold increase in AR's association relative to EGF. The analysis was performed for (**a**) gefitinib and (**b**) cetuximab with the base model parameters. (**c** and **d**) The simulations in panels (**a**) and (**b**) were repeated but with (**c**) the rate constants for phosphorylation within ligand-bound dimers ($k_{p,L}$) and dephosphorylation at the cell surface and in the cell interior ($k_{dp,s}$ and $k_{dp,i}$, respectively) reduced by 100-fold and (**d**) the rate constants for receptor dimerization at the cell surface and in the cell interior ($k_{d,fs}$ and $k_{d,fi}$, respectively) and uncoupling of ligand-bound receptor dimers ($k_{d,rL}$) reduced by 10^3-fold, respectively. For panels (**a–d**), the grey scale colorbars at left show the percent of phosphorylated EGFR (pEGFR) in the absence of drug as a function of ligand cycling factor. The $\log_{10}(IC_{50})$, with IC_{50} in μmol/l units, as a function of ligand and drug cycling factors is shown in colored contour plots, with the color scale shown at right of each contour.

constants for EGFR-cetuximab binding ($k_{c,f}$ and $k_{c,r}$), and rate constants for EGFR internalization and sorting (k_i and k_x) (**Figure 4b**). Competition of cetuximab with ligand for EGFR binding explains sensitivity to cetuximab and EGF binding parameters. Sensitivity to k_i and k_x arises because cetuximab binds EGFR at the cell surface, and these parameters control EGFR distribution between the cell surface and interior. $IC_{50}^{E,c}$ is insensitive to perturbations in $k_{p,L}$, $k_{dp,s}$, or $k_{dp,i}$ because cetuximab indirectly disrupts receptor phosphate cycling by preventing receptor monomers from dimerizing. Relatively slow dephosphorylation is sufficient to reduce receptor phosphorylation in this context. For 1.6 nmol/l AR ($IC_{50}^{A,c}$), we observe sensitivity mainly to the cetuximab binding parameters (**Figure 4b**), which arises because EGFR occupancy is so low that perturbations in AR binding constants cannot promote substantial competition with cetuximab. $IC_{50}^{A,c}$ is relatively insensitive to perturbations in k_i and k_x because there is little EGFR internalization for this AR concentration. Increasing AR concentration sensitizes $IC_{50}^{A,c}$ to ligand binding and trafficking parameters, as binding and endocytosis become more robust with the larger AR concentration (**Figure 4b**).

Note that parameter sensitivity results are not shown in **Figure 4** for perturbations to EGFR, GRB2, or ATP concentrations because results for those simulations reflect effects already shown through variations in the parameters that control process steps in which those species are involved. For example, the relative importance of changing EGFR expression is reflected by results for perturbations in receptor dimerization parameters.

Kinetics of therapeutic-mediated reductions in EGFR phosphorylation

Our results suggest that some differences in gefitinib and cetuximab IC_{50} determinants arise because the kinetics with which phosphorylated receptors become dephosphorylated (and eventually rephosphorylated) in the presence of drugs influence IC_{50}. This dependence arises because of the small time scales for the many reversible processes considered relative to receptor lifetime, and such effects can be observed in calculations of EGFR phosphorylation response to therapeutics. For example, the relative insensitivity of cetuximab IC_{50} to dephosphorylation kinetics can be elucidated by considering predicted receptor dephosphorylation kinetics in response to cetuximab versus gefitinib after an initial ligand pulse (**Figure 5a**). Gefitinib reduces EGFR phosphorylation more rapidly than an equimolar dose of cetuximab, as indicated by

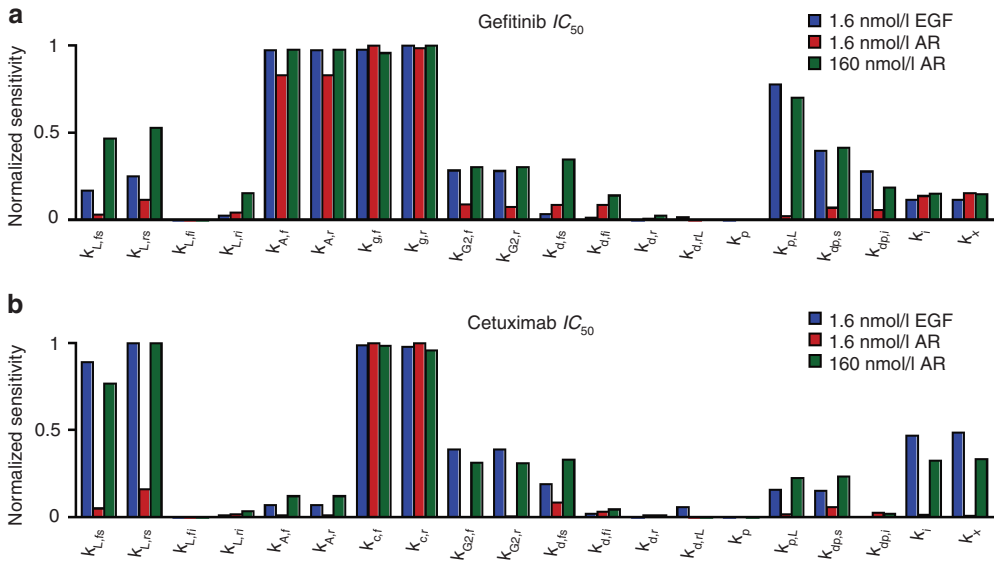

Figure 4 Local sensitivity analysis to identify determinants of IC_{50} for gefitinib and cetuximab. (**a** and **b**) Sensitivity of IC_{50} values to perturbations of 10-fold in each of the model parameters was computed for (**a**) gefitinib or (**b**) cetuximab. Sensitivities were reported as the absolute value of the difference in the logarithm of the base IC_{50} and the perturbed IC_{50} values and then normalized to the maximum. This analysis was performed for 1.6 nmol/l epidermal growth factor (EGF), 1.6 nmol/l amphiregulin (AR), and 160 nmol/l AR.

time scales for phosphorylated EGFR reductions (t_{50}) of 0.2 and 7.7 min, respectively. These differences arise because cetuximab competes with relatively slow dimer uncoupling and ligand dissociation processes, while gefitinib competes with relatively rapid ATP dissociation. Thus, reducing EGFR internalization, to ensure EGFR access to cetuximab, and increasing ligand cycling, which promotes dimer uncoupling, produces nearly identical gefitinib and cetuximab t_{50} values (**Figure 5b**). For 1.6 nmol/l or 160 nmol/l AR, the predicted t_{50} values are similar for the therapeutics because AR cycles more rapidly than EGF (**Figure 5c,d**).

To further identify processes that influence the time scales with which therapeutics reduce receptor phosphorylation, we performed parameter sensitivity analyses for t_{50} calculations (**Figure 5e,f**). The t_{50} for 1.6 nmol/l EGF and 1 μmol/l gefitinib ($t_{50}^{E,g}$) is sensitive to perturbations in $k_{dp,s}$ and $k_{dp,i}$, $k_{p,L}$, $k_{A,f}$ and $k_{A,r}$, $k_{g,f}$ and $k_{g,r}$, k_i, and parameters for GRB2-EGFR binding ($k_{G2,f}$ and $k_{G2,r}$) (**Figure 5e**). Sensitivity to $k_{G2,f}$, $k_{G2,r}$, and k_i is observed because GRB2 binding protects tyrosines from dephosphorylation and because the endosomal compartment is characterized by different kinetics for processes leading to receptor phosphorylation and dephosphorylation. The t_{50} for 1.6 nmol/l AR and 1 μmol/l gefitinib ($t_{50}^{A,g}$) is most sensitive to perturbations in $k_{dp,s}$, $k_{dp,i}$ and $k_{G2,f}$ and $k_{G2,r}$. $t_{50}^{A,g}$ is less sensitive to perturbations in $k_{p,L}$ than $t_{50}^{E,g}$ because of a reduced dimerization driving force in the presence of AR. For 160 nmol/l AR, $t_{50}^{A,g}$ sensitivity to perturbations in $k_{p,L}$ increases but is still lower than that for 1.6 nmol/l EGF due to rapid AR dissociation.

The t_{50} for 1.6 nmol/l EGF and 1 μmol/l cetuximab ($t_{50}^{E,c}$) is most sensitive to changes in $k_{L,fs}$, $k_{L,rs}$, $k_{G2,f}$, $k_{G2,r}$, $k_{dp,i}$, k_i, and k_x (**Figure 5f**). Compared to $t_{50}^{E,g}$, $t_{50}^{E,c}$ is less sensitive to perturbations in dephosphorylation parameters and more sensitive to perturbations in ligand binding parameters because ligand dissociation is more rate-limiting for cetuximab-mediated reductions in EGFR phosphorylation than tyrosine dephosphorylation. The t_{50} for 1.6 nmol/l AR and 1 μmol/l cetuximab ($t_{50}^{A,c}$) is most sensitive to changes in $k_{c,f}$, $k_{G2,f}$, $k_{G2,r}$, $k_{dp,s}$, and $k_{dp,i}$. Since AR-EGFR dissociation is more rapid than EGF-EGFR dissociation, dephosphorylation is more rate-limiting for cetuximab-mediated reduction in EGFR phosphorylation in the presence of 1.6 nmol/l AR than 1.6 nmol/l EGF. For 160 nmol/l AR, $t_{50}^{A,c}$ is sensitive to perturbations in ligand binding parameters, $k_{c,f}$, GRB2 binding parameters, dephosphorylation parameters, and k_i. Increasing the AR concentration tends to promote receptor dimerization and phosphorylation, but does not promote receptor internalization as efficiently as 1.6 nmol/l EGF. Thus, $t_{50}^{A,c}$ remains sensitive to $k_{dp,s}$ perturbations.

We repeated this analysis for 50 nmol/l gefitinib or cetuximab to explore differences that may arise with drug concentrations at the lower end of those reported *in vivo*[15] (**Supplementary Figure S1a,b**). Relative sensitivity to perturbations in parameters for binding of therapeutics and binding processes with which therapeutic binding competes were increased at these lower drug concentrations due to the fact that drugs are in greater competition for binding to receptors when drug concentrations are reduced. Many of the other parameter sensitivities that were observed for 1 μmol/l drug concentrations were also observed here.

Predicted effects of gefitinib and cetuximab in combination

The clinical utility of combining cetuximab with erlotinib is the focus of ongoing clinical trials (e.g., clinicaltrials.gov ID: NCT00397384). Because our analysis highlights how gefitinib and cetuximab antagonize EGFR phosphorylation through different mechanisms, we used the model to predict the effects of combining cetuximab and gefitinib. For a particular cetuximab or gefitinib concentration, the model predicts that

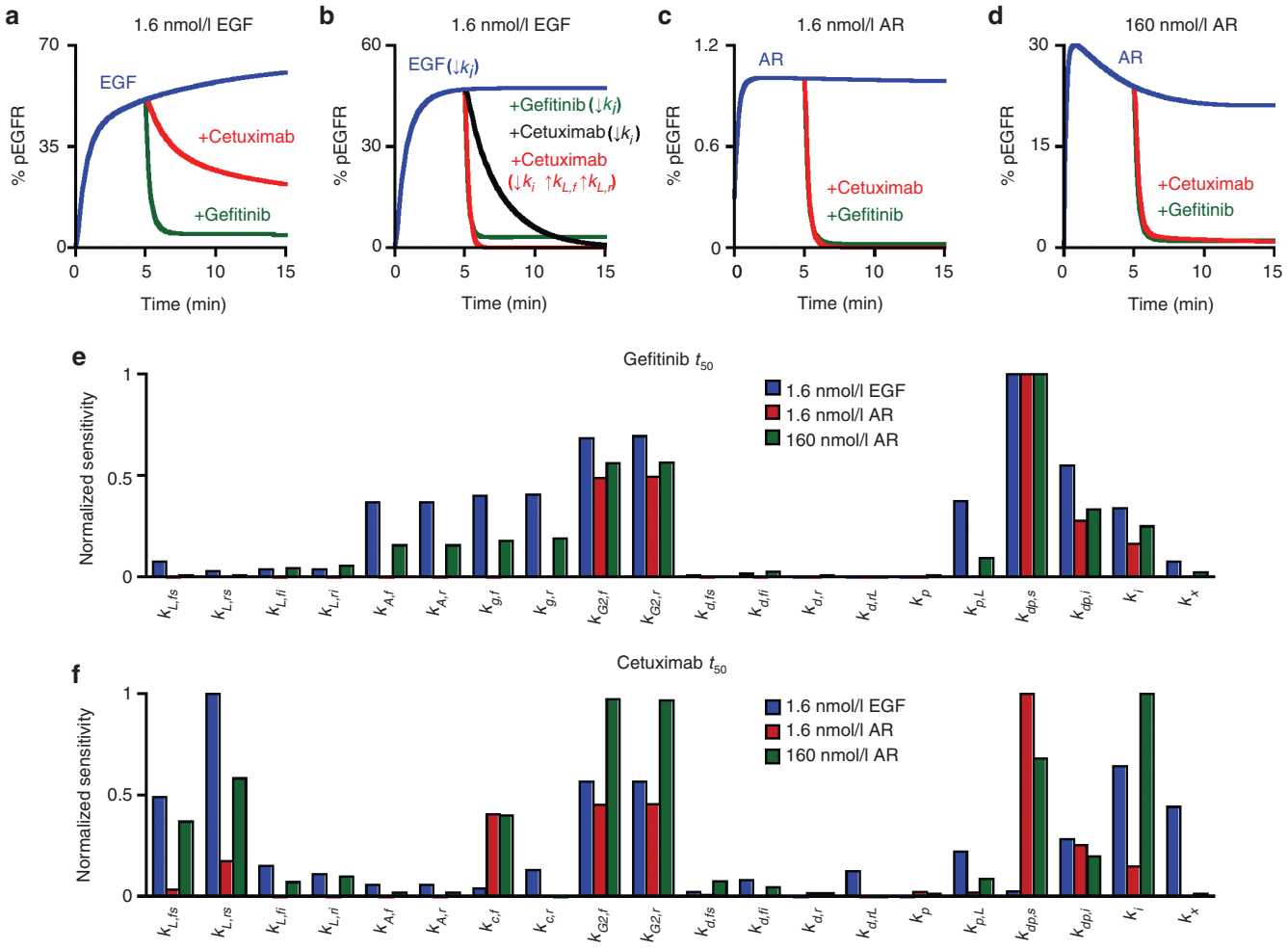

Figure 5 Prediction of and local sensitivity analyses for the time scale with which gefitinib and cetuximab drive epidermal growth factor receptor (EGFR) dephosphorylation. The model was used to predict the percent of phosphorylated EGFR (% pEGFR) observed in response to a 5 min treatment with (**a** and **b**) 1.6 nmol/l EGF, (**c**) 1.6 nmol/l amphiregulin (AR), or (**d**) 160 nmol/l AR, followed by a chase with 1 μmol/l gefitinib or cetuximab. For (**b**), the internalization rate constant (k_i) was set to zero at $t = 0$ min for all conditions and the rate constants for ligand-receptor association and dissociation ($k_{L,f}$ and $k_{L,r}$, respectively) were increased by 100-fold for the cetuximab condition at $t = 5$ min. (**e** and **f**) Sensitivity of t_{50} values to perturbations of 10-fold in each of the model parameters was computed for (**e**) gefitinib or (**f**) cetuximab. Sensitivities were reported as the absolute value of the difference in the logarithm of the base t_{50} and the perturbed t_{50} and then normalized to the maximum. Sensitivity analyses were performed for 1.6 nmol/l EGF, 1.6 nmol/l AR, and 160 nmol/l AR and 1 μmol/l therapeutic.

addition of the other therapeutic further decreases steady-state EGFR phosphorylation in the presence of EGF or AR (**Figure 6a–c**). For our model structure, these effects are not synergistic (**Figure 6d–f**). In fact, negative synergies are predicted for all combinations, resulting from redundant effects that are most apparent at high drug concentrations. The most efficient cotreatments would minimize receptor phosphorylation and redundant effects, while using the lowest drug concentrations to avoid off-target toxicity. With this in mind, we estimated combination efficiency by scaling pEGFR, synergy, and the logarithm of the total drug concentration between 0 and 1 and summing these values for each combination (**Figure 6g–i**). This calculation provides new perspectives for how to combine cetuximab and gefitinib optimally. For example, consider the effects of increasing gefitinib concentration for a fixed cetuximab concentration at 1.6 nmol/l EGF. Starting from ~8 nmol/l cetuximab and 10^{-1} nmol/l gefitinib and increasing gefitinib, efficiency initially decreases until a ~20 nmol/l gefitinib because pEGFR levels are not significantly affected until that point. Beyond ~20 nmol/l gefitinib, efficiency increases beyond its starting point as pEGFR decreases. Efficiency eventually decreases again as drug effects become increasingly redundant. Similar effects occur for AR, but with shifts in efficiency values over the concentration space due to AR's differential ability to drive receptor phosphorylation.

DISCUSSION

Our finding that the abilities of cetuximab and gefitinib to antagonize EGFR phosphorylation are determined by processes beyond those describing equilibrium drug binding motivates new consideration of optimal design strategies for EGFR-targeted therapeutics. To the extent that EGFR phosphorylation level correlates with clinical efficacy, these results also identify possible factors that could underlie the differential effectiveness of the therapeutics among patients.

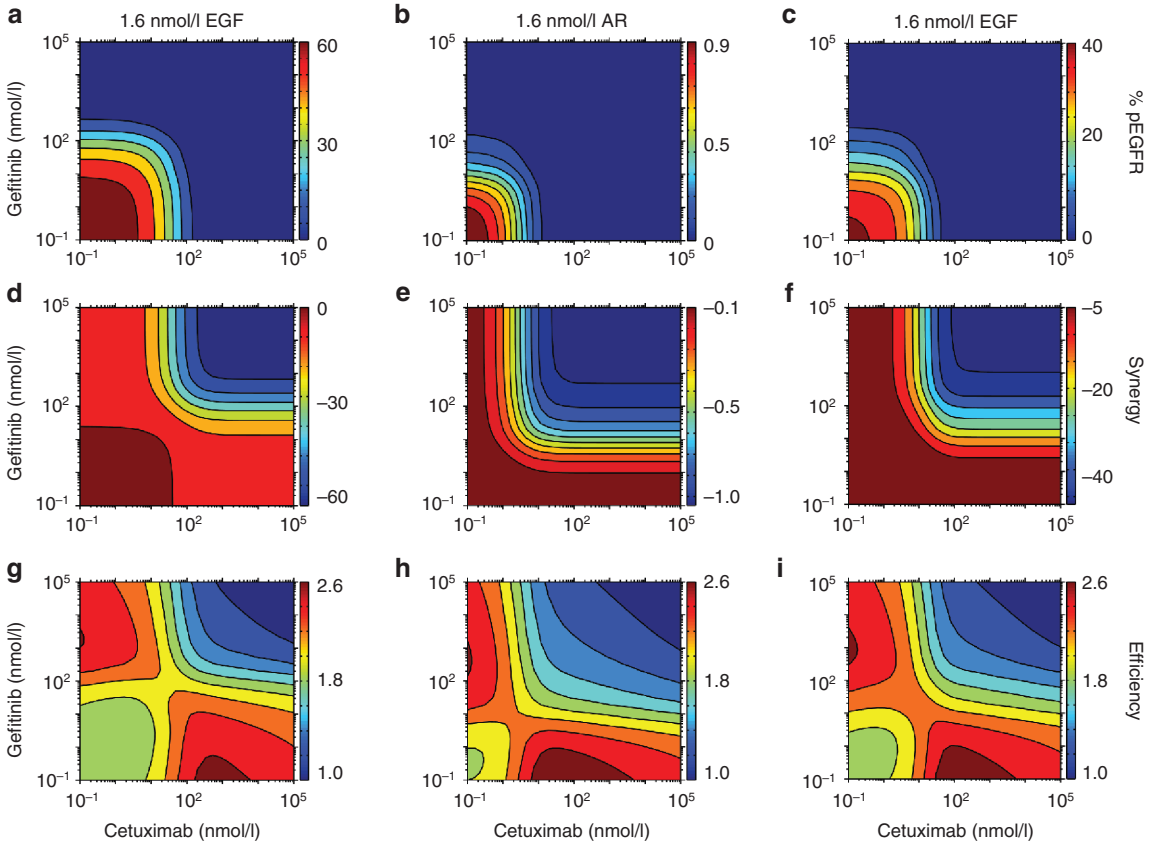

Figure 6 Effects of gefitinib and cetuximab cotreatment. (**a–c**) The model was used to predict the steady-state percent of phosphorylated epidermal growth factor receptor (pEGFR) as a function of cetuximab and gefitinib concentrations for (**a**) 1.6 nmol/l EGF, (**b**) 1.6 nmol/l amphiregulin (AR), or (**c**) 160 nmol/l AR. (**d–f**) Synergy, defined as the reduction in receptor phosphorylation resulting from cotreatment minus the reductions in receptor phosphorylation following treatment with each therapeutic alone, was calculated as a function of cetuximab and gefitinib concentrations for the same ligand concentrations as in (**a–c**). (**g–i**) To estimate therapeutic efficiency, pEGFR (**a–c**), synergy (**d–f**), and the logarithm of the sum of the drug concentrations were scaled to each range between 0 and 1 and then summed for all drug combinations. Based on this definition, therapeutic efficiency is highest for low pEGFR, high synergy, and low amount of drug.

Of course, a number of limitations should be kept in mind in considering the implications of our results. Our analysis implicitly assumes that decreased EGFR phosphorylation will produce more effective therapeutic results. Of course, EGFR transduces signals through numerous pathways, and the integrated effects ultimately determine phenotypic outcomes.[16] Given that receptor–adaptor association is required for downstream signaling, however, computing the IC_{50} for EGFR-GRB2 complex formation may provide additional insight. Interestingly, the relatively rapid kinetics of EGFR-GRB2 binding,[17] which may not prevail for all EGFR adaptors, produces EGFR-GRB2 complex sensitivity results that are indistinguishable from those for phosphorylated receptor (**Supplementary Figure S2a–d**). Of course, our analysis also neglects the potential importance of antibody-mediated cytotoxicity and kinase inhibitor off-target effects. These limitations notwithstanding, a number of novel inferences can be drawn from our results.

Our identification of EGFR dephosphorylation kinetics as a key determinant of therapeutic biochemical efficacy is intriguing given that the activities of protein tyrosine phosphatases that regulate EGFR are altered in certain cancer settings.[18] For example, the receptor-like phosphatase protein tyrosine phosphatase receptor-type S (PTPRS) was found deleted in ~25% of head and neck squamous cell carcinomas.[19] PTPRS deletion was associated with elevated EGFR phosphorylation in tumor tissues, and PTPRS knockdown augmented resistance to erlotinib in head and neck squamous cell carcinomas cell lines. Interestingly, head and neck squamous cell carcinomas cell lines displaying cetuximab resistance also displayed decreased PTPRS expression. Our model does predict some cetuximab IC_{50} dependence on EGFR dephosphorylation kinetics, but it also predicts that other factors are stronger determinants of cetuximab's ability to reduce EGFR phosphorylation.

Our results also predict IC_{50} dependence on the rates of drug and ligand association and dissociation, even for constant affinities. Our prediction that slowing EGFR-gefitinib binding and dissociation cycling decreases IC_{50} is consistent with the observation that slower erlotinib cycling promotes growth inhibition of lung and brain cancer cells.[20] Importantly, Barkovich *et al.*[20] noted that slower erlotinib cycling did not correlate with reduced EGFR phosphorylation, possibly due to the relatively high concentrations of erlotinib required for an effect on cell growth. Our prediction that ligand association and dissociation kinetics affect IC_{50} suggests that different EGFR ligands, which may bind

EGFR with different kinetics,[21] may result in different therapeutic IC_{50} values. Relative mRNA levels of different EGFR ligands generally vary among cells, as in gastric and colon cancer cell lines.[22] Thus, variable therapeutic responses among cells or tumors could be partially related to differential ligand expression profiles.

While our model predicts cetuximab IC_{50} sensitivity to k_i perturbations, only modest k_i sensitivity is predicted for gefitinib (**Figure 4a**). This occurs because cetuximab binds EGFR only at the cell surface, while gefitinib is available to EGFR in both cellular compartments. This is interesting to consider in light of findings that increased EGFR internalization, driven by *ERK2* amplification, can increase the IC_{50} for WZ4002, an irreversible EGFR inhibitor, in PC9 cells.[23] The basis for this effect remains unknown, but it could result from lower protein tyrosine phosphatase activity against EGFR in the endosomal compartment versus the membrane in PC9 cells. In that scenario, increasing receptor internalization would increase gefitinib IC_{50}. Interestingly, cetuximab resistance correlates with increased EGFR ubiquitination in colorectal cancer cells generated through prolonged cetuximab exposure,[24] which could also be related to EGFR internalization effects.[25] Other studies have linked impaired EGFR internalization with cetuximab resistance.[26] Such inconsistencies may occur because endocytosis perturbations can arise for a variety of reasons, with varied consequences for downstream signaling.

METHODS

Model topology

A kinetic model of EGFR phosphorylation at a representative tyrosine was implemented using a framework similar to one previously described,[27] but with several alterations. The updated model includes kinetics for cetuximab binding to EGFR's extracellular domain and for intracellular GRB2 binding to the phosphorylated receptor, and assumes that GRB2-bound receptors internalize at experimentally measured rates for EGFR endocytosis.[27] Note that data for EGFR Y1068 dynamics are used for model training (described below), and that EGFR Y1068 is the primary GRB2 binding site in the EGFR cytoplasmic tail.[28] The model considers cell surface and interior compartments (**Figure 1a**), with the interior (endosomal) volume modeled as before.[27] In each compartment, EGFR monomers reversibly bind ligands and ATP and homodimerize. Ligands and ATP also reversibly bind receptor dimers. Dimerized, ATP-bound receptors undergo phosphorylation characterized by rate constants k_p or $k_{p,L}$, depending on receptor-ligand occupancy. In the surface compartment, phosphorylated receptors are dephosphorylated or bind GRB2, which plays a general adaptor role because of its signaling and endocytosis functions.[29,30] GRB2-bound receptors in the surface compartment irreversibly move to the endosome.[29] Dephosphorylation at the cell surface and in the cell interior are characterized by parameters $k_{dp,s}$ and $k_{dp,i}$, respectively. Rules for model reactions are further explained in **Supplementary Materials**. Model parameters are provided in **Table 1**.

Asymmetric receptor dimers

In our previous model,[27] only symmetric receptor dimerizations were permitted (e.g., a ligand-bound EGFR could only dimerize with another ligand-bound EGFR) to limit model combinatorial complexity. In the updated model, we allowed for asymmetric dimerization with respect to ligand occupancy to reflect an updated structural understanding of dimers.[31]

EGFR-therapeutic binding

Gefitinib is assumed to compete with ATP regardless of EGFR localization. The model assumes that cetuximab binds only surface-localized non-ligand-bound EGFR monomers.[3] Cetuximab is modeled as a monovalent binder of EGFR to focus on a more straightforward comparison between drugs that compete with single ligand or ATP binding events in the extracellular or intracellular compartments, respectively, but the slightly enhanced binding affinity observed for the bivalent full-length antibody[32] was used in model parameterization. Note that monovalent cetuximab fragments potently reduce EGFR phosphorylation in cultured cells.[32] Cetuximab-bound species are permitted to internalize, but cetuximab dissociation is not permitted in the endosome by considering numerical issues. Given that EGFR–cetuximab dissociation and endosomal exit rate constants are of similar magnitude (**Table 1**), this assumption should not significantly affect model predictions.

The model allows cetuximab and gefitinib to antagonize phosphorylation through processes beyond the static sequestration of EGFR from entering the overall path leading to phosphorylation. For example, cetuximab can bind to phosphorylated receptors generated through uncoupling of phosphorylated dimers and dissociation of ligand (**Figure 1b**), preventing receptors from re-dimerizing and -phosphorylating after dephosphorylation. Similarly, gefitinib can bind phosphorylated receptors after ADP dissociation, antagonizing further rounds of phosphorylation (**Figure 1b**).

EGFR ligands

EGF binding constants were based on experimental measurements.[21,33] AR was assumed to dissociate from EGFR 100 times faster than EGF, based on studies suggesting that AR has a larger dissociation constant (K_D),[34] is 50–300 times less potent in cell growth assays,[35] and less efficiently promotes EGFR phosphorylation, CBL association, and ubiquitination.[36] Ligand binding affinities were assumed in the endosome due to the known effects of reduced pH in that compartment.[21] With the differences in ligand binding kinetics for EGF and AR, our model recapitulates published experimental findings that AR is much less efficient than EGF in promoting EGFR endocytosis,[37] with model-predicted specific rate constants for receptor endocytosis of 0.01 or 0.13 min^{-1} for 1.6 nmol/l AR or EGF, respectively.

Comparing therapeutics

For fixed concentration comparisons, we assumed 1 μmol/l or 50 nmol/l for gefitinib and cetuximab. 1 μmol/l significantly exceeds the binding constant of either therapeutic with EGFR (2.1 nmol/l for gefitinib and 5.2 nmol/l for cetuximab)[1,38] and is consistent with some reports of achievable therapeutic concentrations *in vivo*.[39,40] 50 nmol/l concentrations were used in some calculations to span the range of concentrations reported *in vivo*.[15]

Inhibition curves and IC_{50} calculations

We defined IC_{50} as the therapeutic concentration at which steady EGFR phosphorylation was reduced to half its value in the absence of therapeutic, a definition used in other studies (e.g., ref. 41). Inhibition curves were simulated by computing steady EGFR phosphorylation in the presence of ligand over a range of therapeutic concentrations. In making these calculations, we lumped all phosphorylated receptors regardless of binding partners or localization. EGFR degradation and synthesis were not considered due to the computationally intensive algorithm needed to determine the synthesis rate with the specific model structure implemented here.[27]

Pulse-chase curves and t_{50} calculation

To quantify the rate with which therapeutics reduce EGFR phosphorylation, we simulated 5 min treatments of cells with ligands followed by 1 µmol/l or 50 nmol/l therapeutic chases. t_{50} is defined as the time required for 50% of the maximum possible reduction in EGFR phosphorylation. For these calculations, EGFR degradation was not permitted in order to reach a steady state.

Sensitivity analysis

To quantify the relative importance of receptor-level processes in determining IC_{50} and t_{50}, we computed sensitivities to model parameter perturbations. Sensitivity was defined as the absolute value of the difference in the logarithm of IC_{50} or t_{50} values between the perturbed and base parameter values, summed over all perturbations with parameters perturbed by 10- or 0.1-fold.

Model training

To capture realistic EGFR dephosphorylation kinetics, we fit $k_{dp,s}$ and $k_{dp,i}$ using our published data for EGFR Y1068 phosphorylation response to EGF, pervanadate, and gefitinib (**Supplementary Figure S3a–c**), as previously described.[27] Twenty fits were run, with small variations among results. The $k_{dp,s}$ and $k_{dp,i}$ values producing the lowest residual were chosen (**Table 1**). These values were slightly increased compared to those in our previous study,[27] due to the updated model's consideration of GRB2 binding to EGFR, which protects EGFR phosphotyrosines from dephosphorylation.

Representative cell

Cells were assumed to express 5.0×10^4 EGFR[42] and 2.1×10^5 GRB2.[43] ATP concentration was assumed to be 1 mmol/l.[44] EGFR internalization was assumed to be consistent with a specific endocytosis rate constant of 0.13 min^{-1},[45] using an algorithm described previously.[27]

Acknowledgments. This work was supported in part by grant IRG-78-002-30 from the American Cancer Society and by funding to M.J.L. from the University of Pennsylvania. We also thank Janine Buonato for review of the manuscript.

Author Contributions. C.S.M. and M.J.L. designed the research, analyzed the data, and wrote the manuscript. C.S.M. performed the research.

Conflicts of Interest. The authors declared no conflicts of interest.

Study Highlights

WHAT IS THE CURRENT KNOWLEDGE ON THE TOPIC?

✓ Our current understanding of differential response to EGFR-targeted therapeutics is based mainly on understanding of the effects of receptor and other oncogene mutations, but cell-to-cell variability in the processes that regulate EGFR phosphorylation could also give rise to differential response to EGFR-targeted therapy.

WHAT QUESTION DID THIS STUDY ADDRESS?

✓ Our study provides a new quantitative modeling framework and analysis to predict the most important processes determining the ability of EGFR-targeted antibodies and kinase inhibitors to antagonize EGFR phosphorylation.

WHAT THIS STUDY ADDS TO OUR KNOWLEDGE

✓ Our results demonstrate that different kinds of cell-to-cell heterogeneity (e.g., in the activity of phosphatases regulating EGFR) may preferentially contribute to variable response for different classes of EGFR-targeted therapeutics.

HOW THIS MIGHT CHANGE CLINICAL PHARMACOLOGY AND THERAPEUTICS

✓ Our study provides a number of new testable hypotheses for the basis of heterogeneous response to EGFR-targeted therapeutics, the exploration of which may lead to new therapeutic targets and new biomarkers for the stratification of patients for predicted response to EGFR-targeting drugs.

1. Wakeling, A.E. *et al.* ZD1839 (Iressa): an orally active inhibitor of epidermal growth factor signaling with potential for cancer therapy. *Cancer Res.* **62**, 5749–5754 (2002).
2. Pollack, V.A. *et al.* Inhibition of epidermal growth factor receptor-associated tyrosine phosphorylation in human carcinomas with CP-358,774: dynamics of receptor inhibition in situ and antitumor effects in athymic mice. *J. Pharmacol. Exp. Ther.* **291**, 739–748 (1999).
3. Li, S., Schmitz, K.R., Jeffrey, P.D., Wiltzius, J.J., Kussie, P. & Ferguson, K.M. Structural basis for inhibition of the epidermal growth factor receptor by cetuximab. *Cancer Cell* **7**, 301–311 (2005).
4. Kobayashi, T. *et al.* A phase II trial of erlotinib in patients with EGFR wild-type advanced non-small-cell lung cancer. *Cancer Chemother. Pharmacol.* **69**, 1241–1246 (2012).
5. Lu, Y., Liang, K., Li, X. & Fan, Z. Responses of cancer cells with wild-type or tyrosine kinase domain-mutated epidermal growth factor receptor (EGFR) to EGFR-targeted therapy are linked to downregulation of hypoxia-inducible factor-1alpha. *Mol. Cancer* **6**, 63 (2007).
6. Van Schaeybroeck, S. *et al.* Chemotherapy-induced epidermal growth factor receptor activation determines response to combined gefitinib/chemotherapy treatment in non-small cell lung cancer cells. *Mol. Cancer Ther.* **5**, 1154–1165 (2006).
7. Hendriks, B.S. *et al.* Decreased internalisation of erbB1 mutants in lung cancer is linked with a mechanism conferring sensitivity to gefitinib. *Syst. Biol. (Stevenage).* **153**, 457–466 (2006).
8. Araujo, R.P., Petricoin, E.F. & Liotta, L.A. A mathematical model of combination therapy using the EGFR signaling network. *Biosystems.* **80**, 57–69 (2005).
9. Lange, F., Rateitschak, K., Kossow, C., Wolkenhauer, O. & Jaster, R. Insights into erlotinib action in pancreatic cancer cells using a combined experimental and mathematical approach. *World J. Gastroenterol.* **18**, 6226–6234 (2012).

10. Naruo, Y. *et al.* Epidermal growth factor receptor mutation in combination with expression of MIG6 alters gefitinib sensitivity. *BMC Syst. Biol.* **5**, 29 (2011).
11. Purvis, J., Ilango, V. & Radhakrishnan, R. Role of network branching in eliciting differential short-term signaling responses in the hypersensitive epidermal growth factor receptor mutants implicated in lung cancer. *Biotechnol. Prog.* **24**, 540–553 (2008).
12. Cheng, Y. & Prusoff, W.H. Relationship between the inhibition constant (K1) and the concentration of inhibitor which causes 50 per cent inhibition (I50) of an enzymatic reaction. *Biochem. Pharmacol.* **22**, 3099–3108 (1973).
13. Knight, Z.A. & Shokat, K.M. Features of selective kinase inhibitors. *Chem. Biol.* **12**, 621–637 (2005).
14. Ercan, D. *et al.* Amplification of EGFR T790M causes resistance to an irreversible EGFR inhibitor. *Oncogene* **29**, 2346–2356 (2010).
15. Nakagawa, K. *et al.* Phase I pharmacokinetic trial of the selective oral epidermal growth factor receptor tyrosine kinase inhibitor gefitinib ('Iressa', ZD1839) in Japanese patients with solid malignant tumors. *Ann. Oncol.* **14**, 922–930 (2003).
16. Lazzara, M.J. & Lauffenburger, D.A. Quantitative modeling perspectives on the ErbB system of cell regulatory processes. *Exp. Cell Res.* **315**, 717–725 (2009).
17. Morimatsu, M., Takagi, H., Ota, K.G., Iwamoto, R., Yanagida, T. & Sako, Y. Multiple-state reactions between the epidermal growth factor receptor and Grb2 as observed by using single-molecule analysis. *Proc. Natl. Acad. Sci. USA* **104**, 18013–18018 (2007).
18. Julien, S.G., Dubé, N., Hardy, S. & Tremblay, M.L. Inside the human cancer tyrosine phosphatome. *Nat. Rev. Cancer* **11**, 35–49 (2011).
19. Morris, L.G. *et al.* Genomic dissection of the epidermal growth factor receptor (EGFR)/PI3K pathway reveals frequent deletion of the EGFR phosphatase PTPRS in head and neck cancers. *Proc. Natl. Acad. Sci. USA* **108**, 19024–19029 (2011).
20. Barkovich, K.J. *et al.* Kinetics of inhibitor cycling underlie therapeutic disparities between EGFR-driven lung and brain cancers. *Cancer Discov.* **2**, 450–457 (2012).
21. French, A.R., Tadaki, D.K., Niyogi, S.K. & Lauffenburger, D.A. Intracellular trafficking of epidermal growth factor family ligands is directly influenced by the pH sensitivity of the receptor/ligand interaction. *J. Biol. Chem.* **270**, 4334–4340 (1995).
22. Wu, W.K., Tse, T.T., Sung, J.J., Li, Z.J., Yu, L. & Cho, C.H. Expression of ErbB receptors and their cognate ligands in gastric and colon cancer cell lines. *Anticancer Res.* **29**, 229–234 (2009).
23. Ercan, D. *et al.* Reactivation of ERK signaling causes resistance to EGFR kinase inhibitors. *Cancer Discov.* **2**, 934–947 (2012).
24. Lu, Y. *et al.* Epidermal growth factor receptor (EGFR) ubiquitination as a mechanism of acquired resistance escaping treatment by the anti-EGFR monoclonal antibody cetuximab. *Cancer Res.* **67**, 8240–8247 (2007).
25. Madshus, I.H. & Stang, E. Internalization and intracellular sorting of the EGF receptor: a model for understanding the mechanisms of receptor trafficking. *J. Cell Sci.* **122**, 3433–3439 (2009).
26. Wheeler, D.L. *et al.* Mechanisms of acquired resistance to cetuximab: role of HER (ErbB) family members. *Oncogene* **27**, 3944–3956 (2008).
27. Monast, C.S., Furcht, C.M. & Lazzara, M.J. Computational analysis of the regulation of EGFR by protein tyrosine phosphatases. *Biophys. J.* **102**, 2012–2021 (2012).
28. Batzer, A.G., Rotin, D., Ureña, J.M., Skolnik, E.Y. & Schlessinger, J. Hierarchy of binding sites for Grb2 and Shc on the epidermal growth factor receptor. *Mol. Cell. Biol.* **14**, 5192–5201 (1994).
29. Jiang, X., Huang, F., Marusyk, A. & Sorkin, A. Grb2 regulates internalization of EGF receptors through clathrin-coated pits. *Mol. Biol. Cell* **14**, 858–870 (2003).
30. Gale, N.W., Kaplan, S., Lowenstein, E.J., Schlessinger, J. & Bar-Sagi, D. Grb2 mediates the EGF-dependent activation of guanine nucleotide exchange on Ras. *Nature* **363**, 88–92 (1993).
31. Liu, P., Cleveland, T.E. 4th, Bouyain, S., Byrne, P.O., Longo, P.A. & Leahy, D.J. A single ligand is sufficient to activate EGFR dimers. *Proc. Natl. Acad. Sci. USA* **109**, 10861–10866 (2012).
32. Fan, Z., Masui, H., Altas, I. & Mendelsohn, J. Blockade of epidermal growth factor receptor function by bivalent and monovalent fragments of 225 anti-epidermal growth factor receptor monoclonal antibodies. *Cancer Res.* **53**, 4322–4328 (1993).
33. Waters, C.M., Overholser, K.A., Sorkin, A. & Carpenter, G. Analysis of the influences of the E5 transforming protein on kinetic parameters of epidermal growth factor binding and metabolism. *J. Cell. Physiol.* **152**, 253–263 (1992).
34. Shoyab, M., Plowman, G.D., McDonald, V.L., Bradley, J.G. & Todaro, G.J. Structure and function of human amphiregulin: a member of the epidermal growth factor family. *Science* **243**, 1074–1076 (1989).
35. Adam, R. *et al.* Modulation of the receptor binding affinity of amphiregulin by modification of its carboxyl terminal tail. *Biochim. Biophys. Acta* **1266**, 83–90 (1995).
36. Stern, K.A., Place, T.L. & Lill, N.L. EGF and amphiregulin differentially regulate Cbl recruitment to endosomes and EGF receptor fate. *Biochem. J.* **410**, 585–594 (2008).
37. Roepstorff, K. *et al.* Differential effects of EGFR ligands on endocytic sorting of the receptor. *Traffic* **10**, 1115–1127 (2009).
38. Patel, D. *et al.* Monoclonal antibody cetuximab binds to and down-regulates constitutively activated epidermal growth factor receptor vIII on the cell surface. *Anticancer Res.* **27**, 3355–3366 (2007).
39. Albanell, J. *et al.* Pharmacodynamic studies of the epidermal growth factor receptor inhibitor ZD1839 in skin from cancer patients: histopathologic and molecular consequences of receptor inhibition. *J. Clin. Oncol.* **20**, 110–124 (2002).
40. Mukohara, T. *et al.* Differential effects of gefitinib and cetuximab on non-small-cell lung cancers bearing epidermal growth factor receptor mutations. *J. Natl. Cancer Inst.* **97**, 1185–1194 (2005).
41. Pedersen, M.W., Pedersen, N., Ottesen, L.H. & Poulsen, H.S. Differential response to gefitinib of cells expressing normal EGFR and the mutant EGFRvIII. *Br. J. Cancer* **93**, 915–923 (2005).
42. Berkers, J.A., van Bergen en Henegouwen, P.M. & Boonstra, J. Three classes of epidermal growth factor receptors on HeLa cells. *J. Biol. Chem.* **266**, 922–927 (1991).
43. Kholodenko, B.N., Demin, O.V., Moehren, G. & Hoek, J.B. Quantification of short term signaling by the epidermal growth factor receptor. *J. Biol. Chem.* **274**, 30169–30181 (1999).
44. Zamaraeva, M.V., Sabirov, R.Z., Maeno, E., Ando-Akatsuka, Y., Bessonova, S.V. & Okada, Y. Cells die with increased cytosolic ATP during apoptosis: a bioluminescence study with intracellular luciferase. *Cell Death Differ.* **12**, 1390–1397 (2005).
45. Lazzara, M.J. *et al.* Impaired SHP2-mediated extracellular signal-regulated kinase activation contributes to gefitinib sensitivity of lung cancer cells with epidermal growth factor receptor-activating mutations. *Cancer Res.* **70**, 3843–3850 (2010).
46. Myers, A.C., Kovach, J.S. & Vuk-Pavlović, S. Binding, internalization, and intracellular processing of protein ligands. Derivation of rate constants by computer modeling. *J. Biol. Chem.* **262**, 6494–6499 (1987).
47. Shan, Y. *et al.* Oncogenic mutations counteract intrinsic disorder in the EGFR kinase and promote receptor dimerization. *Cell* **149**, 860–870 (2012).
48. Hendriks, B.S., Opresko, L.K., Wiley, H.S. & Lauffenburger, D. Quantitative analysis of HER2-mediated effects on HER2 and epidermal growth factor receptor endocytosis: distribution of homo- and heterodimers depends on relative HER2 levels. *J. Biol. Chem.* **278**, 23343–23351 (2003).
49. Fan, Y.X., Wong, L., Deb, T.B. & Johnson, G.R. Ligand regulates epidermal growth factor receptor kinase specificity: activation increases preference for GAB1 and SHC versus autophosphorylation sites. *J. Biol. Chem.* **279**, 38143–38150 (2004).
50. Hendriks, B.S., Opresko, L.K., Wiley, H.S. & Lauffenburger, D. Coregulation of epidermal growth factor receptor/human epidermal growth factor receptor 2 (HER2) levels and locations: quantitative analysis of HER2 overexpression effects. *Cancer Res.* **63**, 1130–1137 (2003).

Supplementary information accompanies this paper on the *CPT: Pharmacometrics & Systems Pharmacology* website (http://www.nature.com/psp)